Synthesis and electrochemical study of 2-(2-pyridyl)benzothiazole complexes with transition metals (Co^{II}, Ni^{II}, and Cu^{II}). Molecular structure of aquabis[2-(2-pyridyl)benzothiazole]copper(II) diperchlorate

E. K. Beloglazkina, I. V. Yudin, A. G. Majouga, A. A. Moiseeva, A. I. Tursina, and N. V. Zyk*

Department of Chemistry, M. V. Lomonosov Moscow State University, 1 Leninskie Gory, 119992 Moscow, Russian Federation. E-mail: bel@org.chem.msu.ru

The reactions of 2-(2-pyridyl)benzothiazole (**1**) with $MX_2 \cdot nH_2O$ salts (M = Ni^{II}, Co^{II}, or Cu^{II}; X = Cl or ClO_4; n = 0—2) in EtOH afforded the corresponding complexes. Depending on the nature of the counterion in the starting metal salt, the reactions give compounds of composition $M(\mathbf{1})Cl_2 \cdot nH_2O$ or $Cu(\mathbf{1})_2(ClO_4)_2 \cdot H_2O$. The molecular and crystal structure of the $Cu^{II}(\mathbf{1})_2(ClO_4)_2 \cdot H_2O$ complex was established by X-ray diffraction. The copper atom in this complex has a distorted tetragonal-pyramidal ligand environment and is coordinated by four nitrogen atoms of two ligand molecules and one water molecule. Electrochemical study of the ligand and the resulting complexes by cyclic voltammetry and at a rotating disk electrode demonstrated that ligand **1** stabilizes reduced forms of complexes containing Ni, Co, or Cu atoms in the oxidation state +1.

Key words: 2-(2-pyridyl)benzothiazole, nickel(II) complexes, cobalt(II) complexes, copper(II) complexes, cyclic voltammetry, molecular and crystal structure.

Nickel(II) and copper(II) complexes with organic S,N-containing ligands can be reversibly reduced to metal(I) complexes; they have attracted attention as functional models of metalloenzymes and electroactive catalysts. From this point of view, 2-(2-pyridyl)benzothiazole (**1**), which contains electron-donating nitrogen and sulfur atoms and is capable of forming chelate five-membered metallacycles upon complexation, is of considerable interest. In the present study, we synthesized Co^{II}, Ni^{II}, and Cu^{II} complexes with 2-(2-pyridyl)benzothiazole.

To use the resulting metal complexes as potential electroactive catalysts, it is necessary that oxidation and reduction or at least their initial steps be electrochemically reversible or quasireversible. Hence, we also studied the electrochemical behavior of the resulting complexes.

Complexes of 2-(2-pyridyl)benzothiazole with transition metal ions are few in number (Pt^{II},[1] Sn^{II},[2] Ru^{III},[3,4] and Re^{V} complexes[5—7]). Ligand **1** can exist in two different conformations (N—S and N—N) and form complexes with one or two ligand molecules. However, all structurally characterized complexes contain only one molecule **1** adopting an N—N conformation, *i.e.*, the metal atom is coordinated through the lone pairs of two nitrogen atoms of the pyridine and benzothiazole fragments. It should be noted that free ligand **1** has an N—S conformation in the crystalline state.[2]

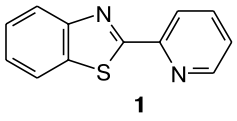

1

N—S Conformation

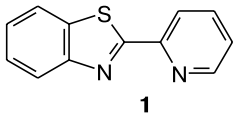

1

N—N Conformation

In the present study, we synthesized Co^{II}, Ni^{II}, and Cu^{II} complexes with 2-(2-pyridyl)benzothiazole and studied their electrochemical properties.

Results and Discussion

Ligand **1** was synthesized from *o*-aminothiophenol and 2-pyridinecarbaldehyde according to a known procedure.[7] Under the reaction conditions, the resulting 2-substituted benzothiazoline is oxidized by atmospheric oxygen to give the corresponding benzothiazole.[8] Complexes **2—5** were synthesized according to Scheme 1.

The composition of the complex depends on the nature of the counterion in the starting metal salt. The reactions with nickel, cobalt, or copper salts containing the nucleophilic chloride anion produce complexes **2—4** containing one ligand fragment regardless of the **1** : MCl_2 ratio. The reaction with the $Cu(ClO_4)_2 \cdot 6H_2O$ salt containing the perchlorate anion affords complex **5** with two

Published in Russian in *Izvestiya Akademii Nauk. Seriya Khimicheskaya,* No. 10, pp. 1738—1744, October, 2006.

1066-5285/06/5510-1803

Scheme 1

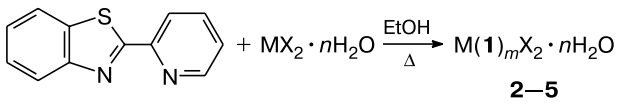

1 **2—5**

Complex	M	*m*	X	*n*
2	Ni	1	Cl	2
3	Co	1	Cl	0
4	Cu	1	Cl	2
5	Cu	2	ClO_4	1

ligand molecules regardless of the ratio of the ligand to the inorganic salt.

Compounds **1—5** were characterized by IR and UV-Vis spectroscopy. In the IR spectra of complexes **1—5**, the C=N absorption band is shifted to higher wavenumbers (1600—1610 cm^{-1}) compared to that of the starting compound **1** (1570 cm^{-1}). This is evidence that the resulting complexes contain ligand **1** in an N—N conformation. The absorption bands at 1300—1500 cm^{-1} belonging to vibrations of the pyridine fragment[9] are also shifted compared to those of benzothiazole **1**, which confirms the involvement of the pyridine nitrogen atom in coordination.[10]

Complexes **1—5** were studied by UV-Vis spectroscopy (Table 1). The ligand is characterized by absorption bands only in the UV region, which correspond to π—π* and n—π* transitions in organic molecules. The formation of the complexes leads to a slight shift and a change in the intensity of these bands. In some cases, additional absorption bands are observed. In the optical spectrum of nickel complex **2**, absorption bands in the visible region are absent, which is evidence for an octahedral coordination of the Ni^{II} atom.[11] Apparently, the metal atom in the latter complex is coordinated by two nitrogen atoms, two chloride anions, and two water molecules.

The optical spectrum of complex **3** shows two bands in the visible region at 588 and 684 nm (ε = 1082 and 1403 mol L^{-1} cm^{-1}, respectively). The latter band is, apparently, a superposition of two absorption bands. This spectral pattern and the extinction coefficients are characteristic of coordination compounds containing the central Co^{II} atom in a tetrahedral ligand environment.[11]

Table 1. UV-Vis spectra of solutions of compounds **1—5** (10^{-3} mol L^{-1}) in MeCN

Compound	λ/nm ($\varepsilon \cdot 10^{-3}$/L mol^{-1} cm^{-1})
1*	261 (6.27), 308 (17.65)
2	271 (8.78), 324 (16.98)
3	253 (9.16), 310 (18.53), 588 (1.08), 684 (1.40)
4	254 (7.59), 314 (17.60)
5	258 (10.80), 333 (19.64)

* The concentration was $1.7 \cdot 10^{-4}$ mol L^{-1}.

Molecular structure of compound 5. The structure of complex **5** was established by X-ray diffraction. Crystals suitable for X-ray diffraction were grown by slow evaporation of a solution of the complex in a 1 : 1 EtOH—$CHCl_3$ mixture. Crystallographic data and the X-ray data collection and refinement statistics are given in Table 2. Selected bond lengths and bond angles are listed in Table 3. The molecular structure of complex **5** is presented in Fig. 1. The X-ray diffraction data show that the organic ligand has an N—N conformation, like compound **1** in the complexes described earlier.[1—7] However, unlike all known 2-(2-pyridyl)benzothiazole complexes with metals, compound **5** contains two ligand fragments. The copper atom in complex **5** has a distorted square-pyramidal environment and is coordinated by four nitrogen atoms of the pyridine and benzoimidazole rings and the oxygen atom of the H_2O molecule. The imidazole and pyridine rings in the ligand fragments are planar and virtually coplanar. Two molecules of the organic ligand in complex **5**

Table 2. Crystallographic data and X-ray data collection and refinement statistics for compound **5**

Parameter	Characteristics
Molecular formula	$C_{24}H_{18}Cl_2CuN_4O_9S_2$
Molecular weight	704.98
Color, crystal shape	Dark-green prisms
Crystal dimensions/mm	0.25×0.22×0.18
Crystal system	Tetragonal
Space group	$I4_1cd$
a/Å	14.6926(11)
c/Å	25.5694(18)
V/Å^3	5519.7(7)
Z	8
d_{calc}/g cm^{-3}	1.697
μ/cm^{-1}	4.853
F(000)	2856
θ range/deg	5.49—74.78
Ranges of reflection indices	$0 \le h \le 18$, $0 \le k \le 18$, $0 \le l \le 32$
Number of measured reflections	2815
Number of independent reflections (R_{int})	1452 (0.0691)
Number of reflections with $I > 2\sigma(I)$	1142
Number of refinement variables	195
Goodness-of-fit on F^2	0.978
R factors based on reflections with $I > 2\sigma(I)$	$R_1 = 0.0655$, $wR_2 = 0.1799$
R factors based on all reflections	$R_1 = 0.0793$, $wR_2 = 0.1995$
Residual electron density (min/max)/e Å^{-3}	−0.50/0.77

Table 3. Selected interatomic distances (d) and bond angles (ω) for compound **5** (atomic numbering scheme corresponds to that used in Fig. 1)

Bond	d/Å	Angle	ω/deg
Cu—N(1)	1.972(6)	N(1)—Cu—N(1)	172.0(5)
Cu—N(2)	2.062(7)	N(1)—Cu—N(2)	101.9(3)
Cu—O	2.111(11)	N(1)—Cu—N(2)	81.6(3)
N(1)—C(3)	1.302(11)	N(2)—Cu—N(2)	128.9(4)
N(1)—C(9)	1.382(11)	N(1)—Cu—O	86.0(2)
S(2)—C(3)	1.716(9)	N(2)—Cu—O	115.5(2)
S(2)—C(5)	1.715(11)	Cu—N(1)—C(3)	114.0(6)
N(2)—C(4)	1.385(11)	Cu—N(1)—C(9)	134.1(6)
C(3)—C(4)	1.452(13)	Cu—N(2)—C(4)	111.5(6)

are arranged in a head-to-head fashion. The mean planes of two ligands in the base of the pyramid intersect at an angle of 50.75(3)°. The copper and oxygen atoms lie on a twofold axis.

Both five-membered chelate rings in complex **5** are almost planar. The copper—nitrogen (pyridine) (2.062 Å) and copper—nitrogen (thiazole) (1.972 Å) distances are similar to those found in other iminopyridine copper complexes.[12—14]

Electrochemical study. Free ligand **1** and complexes **2—5** were studied by cyclic voltammetry (CV) and rotating disk electrode (RDE) voltammetry at glassy-carbon (GC), Pt, and Au electrodes in anhydrous DMF in the presence of a 0.05 M Bu_4NClO_4 solution as the supporting electrolyte. It was found that the potentials are virtually independent of the material of the electrode. Hence, the data obtained at a glassy-carbon electrode (in this case, measurements can be performed in a wider potential range) are considered below. The results of electrochemical study are given in Table 4. The cyclic voltammograms of compounds **1—4** are shown in Fig. 2.

For ligand **1**, no oxidation peaks are observed up to E = +1.7 V. Reduction occurs in three successive steps.

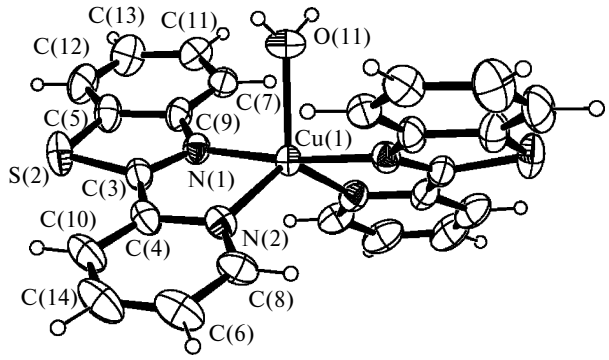

Fig. 1. Molecular structure of compound **5**. The unnumbered atoms are related to the numbered atoms by the symmetry operation $-x + 1, -y, z$. The anisotropic displacement ellipsoids are drawn at the 40% probability level.

Table 4. Electrochemical reduction potentials (E^{Red}) and oxidation potentials (E^{Ox}) of compounds **1—5** measured relative to Ag/AgCl/KCl(satur.) by the CV method (E_p is the peak potential) and using the RDE method ($E_{1/2}$ is the half-wave potential) at a glassy carbon electrode (DMF, 0.05 M Bu_4NClO_4 solution)

Compound	E_p^{Red}	$E_{1/2}^{Red}$	E_p^{Ox}	$E_{1/2}^{Ox}$
	V			
1	−1.72/−1.66, −2.34, −2.80	−1.67 (1), −2.36 (2)	—	—
2	−0.93[a], −1.21/−0.11[c], −1.73/−1.67, −2.28, −2.66	−0.91 (0.5)[b], −1.20 (0.7)[d], −1.73 (0.85), −2.24 (0.3)	1.20	1.10 (2)
3	−1.06/−0.97, −1.43, −1.73/−1.65, −2.34	−1.20 (1), −1.72 (2)[d]	1.25	1.21 (2)
4	0.44/0.54[e], −0.53[f,g], −1.72/−1.65, −2.31, −2.78	0.42 (1), −0.75 (small), −1.71 (1), −2.42 (1.6)	1.19	1.14 (2)
5	0.16/0.24, −0.32/0.22[g], −1.71/−1.61, −2.32, −2.78	0.16 (0.5), −0.35 (0.6), −1.70 (2), −2.32 (4)	—	—
$CoCl_2 \cdot 6H_2O$	−0.86, −1.21/0.35	−1.30	1.53, 1.70	1.50 (1), 1.70 (1)
$NiCl_2 \cdot 6H_2O$	−1.32/0.16	−1.30 (2)	1.20	1.00 (2)
$CuCl_2 \cdot 2H_2O$	+0.45/0.58, −0.51/−0.16	0.50 (1)	—	—
$Ni(ClO_4)_2 \cdot 6H_2O$	−1.25/0.16	−1.70 (0.8)	—	—
$Cu(ClO_4)_2 \cdot 6H_2O$	+0.00/−0.11, −0.18/+0.27	−0.12 (1)	—	—

Note. The peak potentials on the reverse scans of CV curves are given after a slash; the number of electrons transferred in this step is given in parentheses.

[a] The reverse desorption peak at a potential of +0.43 V appears only upon electrolysis for 10—30 s at the potential of this peak.

[b] Apparently, the electrode is covered by Ni^0, and further reduction occurs at the modified electrode, resulting in a decrease in the current of the observed waves and the appearance of a peak at an RDE.

[c] The peak of oxidative desorption of M^0.

[d] A peak instead of the "normal" wave is observed in the RDE curve.

[e] The initial potential was 0.7 V.

[f] A Pt electrode.

[g] The peak is weakly pronounced and is not always reproducible.

The first step corresponds to a one-electron reversible redox transition; the second step, to a two-electron irreversible process (see Fig. 2, *a*). It is known that thiazole and its alkyl and aryl derivatives are not reduced in polarographic measurements. However, the introduction of an

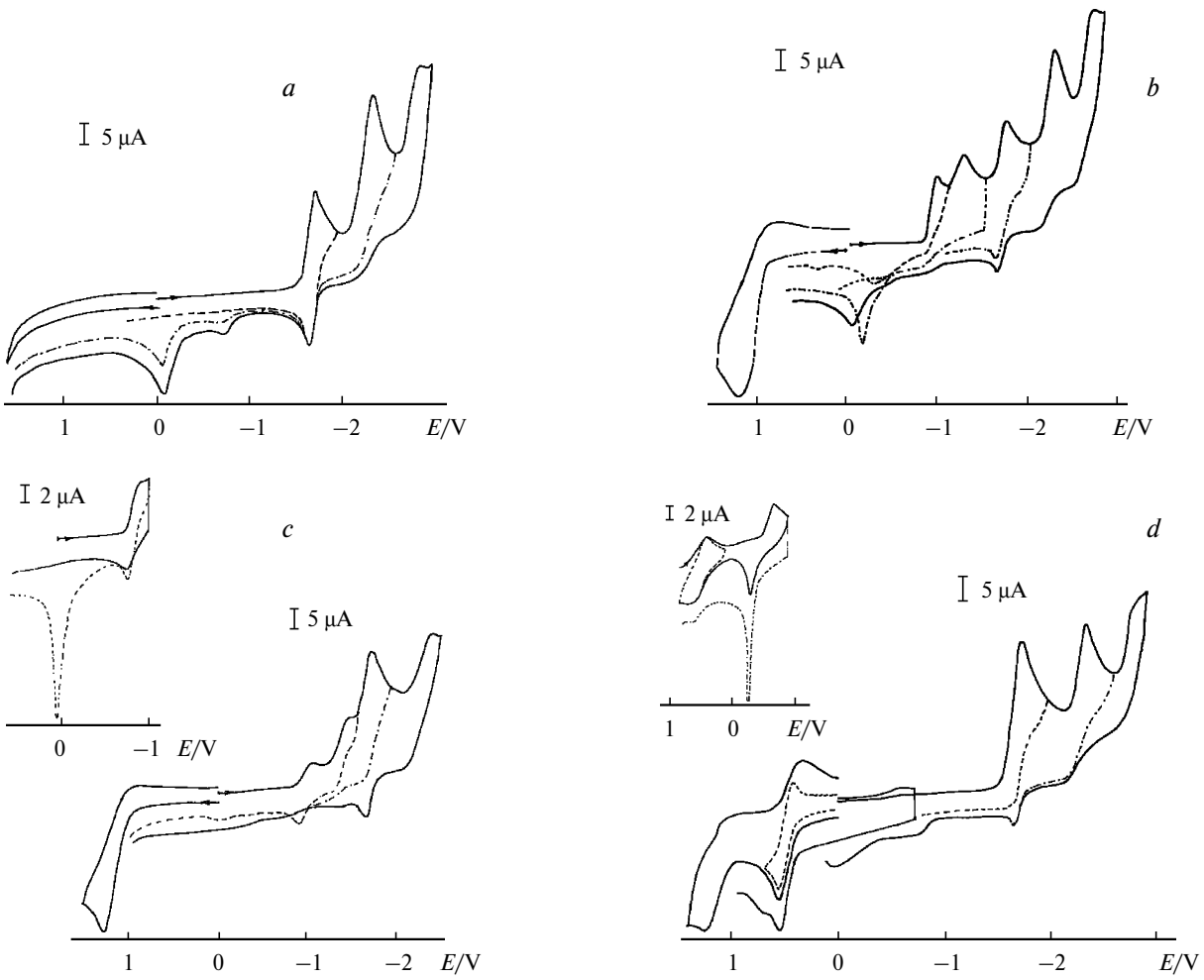

Fig. 2. Cyclic voltammograms of ligand **1** (*a*) and complexes **2** (*b*), **3** (*c*), and **4** (*d*) in DMF. The changes in the intensity of the peak of oxidative desorption of Co^0 (*c*) or Cu^0 (*d*) (at a Pt electrode) during electrolysis at a potential of ~−1 V are shown in the inset.

electron-withdrawing group into the thiazole ring may impart the ability to be reduced at the thiazole ring.[15] Electrochemical reduction of benzothiazolium salts occurs at the N=C bond.[16] Semiempirical calculations by the PM3 method confirmed that the orbitals of the —N=C fragment of the thiazole ring make the main contribution to LUMO of ligand **1**. Therefore, the first reduction step of compound **1** apparently gives rise to the stable radical anion (Scheme 2).

Scheme 2

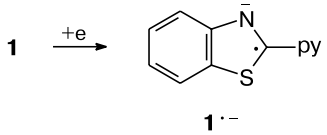

1$^{\bullet -}$

Further two-electron reduction of radical anion **1**$^{\bullet -}$ can occur either again at the thiazole fragment or, which is more probable, at the pyridine ring. It should be noted that unsubstituted pyridine is reduced polarographically at a potential of −2.07 V.[17] The presence of an electron-donating substituent in the pyridine ring hinders reduction, which apparently accounts for more negative reduction potentials (see Table 4).

Compared to the CV curves of free ligand **1**, the CV curves of nickel complex **2** have two additional one-electron peaks in the cathodic region at less negative potentials (see Fig. 2, *b*) than the first peak of the free ligand. Apparently, these peaks correspond to $Ni^{II} \rightarrow Ni^{I}$ and $Ni^{I} \rightarrow Ni^{0}$ transitions. A peak of oxidative desorption of nickel metal from the electrode surface of the characteristic triangular shape is observed on the reverse scan of the voltammogram after the second peak potential. The intensity of this peak substantially increases when electrolysis is performed at the potential of the second reduction peak.[18] The formation of Ni^0 is additionally evidenced by the formation of the visually observed black precipitate at the electrode. The next two peaks in the

cathodic region of the CV curve are attributed to reduction of ligand **1**.

Electrolysis at −1.0 V also gives a peak at E_p = +0.43 V on the reverse anodic scan, and the intensity of the peak increases with increasing electrolysis time. Apparently, this peak corresponds to oxidative desorption of a poorly soluble Ni^I complex from the electrode surface. Adsorption is additionally supported by a decrease in the current in voltammograms measured with the use of an RDE[19,20] (see Table 4).

Stability of Ni^I complexes is determined by the type of the ligand environment, and low-valence states of nickel are generally stabilized by either macrocyclic nitrogen-containing ligands or chelating N,O- or N,S-type ligands.[21,22] In other cases, Ni^{II} complexes are generally reduced to Ni^0 in one two-electron step. Our investigation demonstrated that ligand **1** can stabilize the nickel atom in the oxidation state +1.

Reduction of complex **3** is accompanied by the appearance of two additional early peaks in the cathodic region compared to the pattern typical of reduction of the free ligand (see Table 4 and Fig. 2, *c*). These peaks apparently correspond to successive reduction $Co^{II} \rightarrow Co^I \rightarrow Co^0$. In the CV curve, the first reduction peak is electrochemically reversible. After this peak, the peak of oxidative desorption of metal is not observed on the reverse scan of the voltammogram. However, this peak appears upon electrolysis at $E = -1.1$ V (see Fig. 2, *c*). These data suggest that the Co^I compound, which is formed in the first reduction step, is stable under the experimental conditions for at least 2 s (estimated taking into account the potential scan rate of 0.2 V s^{-1}), but then it undergoes slow disproportionation in solution to form Co^{II} and Co^0 compounds. The latter compound decomposes to give cobalt metal (Scheme 3).

Scheme 3

$$\mathbf{3} \underset{-e}{\overset{+e}{\rightleftharpoons}} Co^I(\mathbf{1})Cl_2 \longrightarrow 1/2\,[\mathbf{3} + Co^0 + \mathbf{1} + 2\,Cl^-]$$

The fact of disproportionation is confirmed by an increase in the intensity of the second reduction peak ($Co^I \rightarrow Co^0$) due to the additional formation of Co^{II}, which also would be reduced at this potential. It should be noted that the peak of oxidative desorption of Co^0 is observed on the reverse scan of the CV curve upon electrolysis at $E = -1.45$ V. However, the intensity of this peak is substantially lower than that observed upon electrolysis at the potential of the first reduction wave. This fact can be attributed to adsorption of the Co^I compound on the surface of solid electrodes[19] analogously to reduction of nickel complex **2**. In addition, the intensity of the anodic peak of the reversible transition $Co^{II} \rightarrow Co^I$ is slightly higher than the intensity of the forward peak, which indicates that adsorption occurs.[20]

For copper complex **4**, the CV curve shows a quasi-reversible reduction peak at E_p = +0.42 V ($Cu^{II} \rightarrow Cu^I$) and a peak at −0.5——0.7 V, which is weakly pronounced, poorly reproducible, and observed only at a Pt electrode (apparently, due to the fact that the electrode surface is blocked by the adsorbed poorly soluble Cu^I compound). Upon electrolysis at −0.75 V, a black Cu^0 precipitate is deposited on the electrode, and anodic dissolution of this precipitate occurs at a potential of +0.50 V (see Table 4 and Fig. 2, *d*). In MeCN, the peak corresponding to the $Cu^I \rightarrow Cu^0$ transition is clearly seen at a potential of −0.65 V along with an intense reverse desorption peak at −0.24 V (see Fig. 2, *d*, the inset). As in the case of complexes **2** and **3**, the next peaks are due to reduction of the organic ligand. Initial two-step reduction of metal is also observed for complex **5**. It should be noted that the potential of anodic dissolution of metal depends both on the nature of the anion involved in the complex and the nature of the solvent and varies from 0.51 to −0.24 V (see Table 4).

Earlier, it has been noted[23] that the Cu^I derivative, which is formed in the first step of polarographic reduction of copper(II) compounds (in particular, of $Cu(ClO_4)_2$) in DMF, is unstable and undergoes disproportionation to form compounds containing Cu^{II} and Cu^0. In other studies (see, for example, Ref. 24 and references cited therein), it was hypothesized that stability of Cu^I complexes in DMF is higher in the presence of donor anions (for example, of Cl^-) in solution. A opposed to the results of the study,[23] investigation of reduction of $Cu(ClO_4)_2 \cdot 6H_2O$, as well as of complexes **4** and **5**, in DMF by the CV method at a potential scan rate of 200 mV s^{-1} revealed two peaks at all three types of electrodes, which correspond to the $Cu^{II} \rightarrow Cu^I$ and $Cu^I \rightarrow Cu^0$ transitions.* Based on the results of the present study, it can be concluded that 2-(2-pyridyl)benzothiazole is a ligand stabilizing metal (nickel, cobalt, and copper) derivatives in the oxidation state +1.

Two-electron oxidation of complexes **2—4** occurs at E = 1.10—1.21 V, *i.e.*, in the region, where oxidation of chloride anions is generally observed. According to the results of quantum-chemical calculations, HOMO of these complexes is localized on the lone electron pairs of the chlorine atoms. Consequently, oxidation of compounds **2—4** should occur at the coordinated chloride anions. This conclusion is confirmed by the fact that oxidation peaks are absent for complex **5** containing no chloride ligands, as well as for free ligand **1**.

Therefore, two first reduction steps of all the complexes under study occur at metal. Then the ligand is

* However, only one wave is observed at an RDE at a potential scan rate of 20 mV s^{-1}.

reduced. Oxidation of complexes **2—4** occurs at the coordinated chloride anion. Complex **5** is not oxidized in the achievable potential region (up to +1.7 V). It should be noted that the M^I complexes that are formed in the first reduction step are poorly soluble, which leads to their deposition on the electrode surface and decreases the intensity of successive steps.

Experimental

The IR spectra were measured on a UR-20 instrument in Nujol mulls. The UV-Vis spectra were recorded on Specord-M40 (200—900 nm) and Helios-α Nicolet (200—1100 nm) instruments in 0.1-cm quartz cells at 20—22 °C. The positive-ion mass spectra (laser ionization) were obtained on a Vision 2000 time-of-flight mass spectrometer (N_2 laser, the wavelength was 336 nm).

Electrochemical studies were carried out on a PI-50-1.1 potentiostat equipped with a PR-8 programmer. Glassy-carbon (d = 2 mm), platinum (d = 3 mm), or gold (d = 1 mm) disks were used as the working electrodes; a 0.05 M Bu_4NClO_4 solution in DMF (or MeCN) served as the supporting electrolyte; Ag/AgCl/KCl(satur.) was used as the reference electrode; a Pt plate was used as an auxiliary electrode. The potentials are given taking into account the iR compensation. The potential scan rates were 200 (CV method) and 20 mV s^{-1} (RDE method). The numbers of electrons transferred in redox processes were determined by comparing the limiting wave current in experiments at an RDE with the current of one-electron oxidation of a ferrocene solution at an equal concentration.

All measurements were carried out under dry argon. The samples were dissolved in a pre-deaerated solvent. Dimethylformamide (high-purity grade) was purified by mixing over freshly calcined K_2CO_3 for four days followed by vacuum distillation first over P_2O_5 and then over anhydrous $CuSO_4$.

Quantum-chemical calculations were carried out with the use of the semiempirical SCF PM3 method,[25] which was extended by including the parameters for all first-row transition metals and selected second- and third-row transition metals. This extended method (PM3(tm)) is implemented in the HyperChem program package (HyperCube, Inc., FL, USA). Geometry optimization of the molecules was performed with a specified convergence gradient of at most 10 kal $Å^{-1}$ mol^{-1}.

Ligand **1** was synthesized according to a known procedure.[7] IR, ν/cm^{-1}: 1585, 1570 (C=N), 1510, 1460, 1435, 1380, 1320.

Synthesis of complexes 2—5 (general procedure). A solution of metal chloride ($NiCl_2 \cdot 6H_2O$, $CoCl_2 \cdot 6H_2O$, or $CuCl_2 \cdot 2H_2O$) (1 mmol) or $Cu(ClO_4)_2 \cdot 6H_2O$ (2 mmol) in a minimum amount of EtOH was added to a hot solution of ligand **1** (0.5 g, 2 mmol) in EtOH (5—7 mL). The solution was refluxed for 1 h. The precipitate that formed upon cooling was filtered off, washed with cold EtOH, and dried in air. The melting points of chlorides **2—4** >300 °C; perchlorate **5** explosively decomposes on heating.

Diaqua[2-(2-pyridyl)benzothiazole]nickel(II) dichloride (2). The yield was 40%, the pale-yellow complex. Found (%): C, 37.97; H, 3.36; N, 7.42. $C_{12}H_8N_2S \cdot NiCl_2 \cdot 2H_2O$. Calculated (%): C, 38.19; H, 3.19; N, 7.42. IR, ν/cm^{-1}: 3100—3400 br, 1610 (C=N), 1500, 1465, 1430, 1380, 1335, 1305.

[2-(2-Pyridyl)benzothiazole]cobalt(II) dichloride (3). The yield was 68%, the pale-brick-colored complex. Found (%): C, 41.71; H, 2.50; N, 8.14. $C_{12}H_8N_2S \cdot CoCl_2$. Calculated: C, 42.23; H, 2.35; N, 8.21. IR, ν/cm^{-1}: 1600 (C=N), 1490, 1465, 1420, 1380, 1330, 1310.

Diaqua[2-(2-pyridyl)benzothiazole]copper(II) dichloride (4). The yield was 85%, the yellow complex. Found (%): C, 37.99; H, 2.99; N, 7.53. $C_{12}H_8N_2S \cdot CuCl_2 \cdot 2H_2O$. Calculated (%): C, 37.60; H, 3.13; N, 7.31. IR, ν/cm^{-1}: 3100—3400 br, 1600 (C=N), 1495, 1465, 1430, 1380, 1335, 1310.

Aquabis[2-(2-pyridyl)benzothiazole]copper(II) diperchlorate (5). The yield was 69%, the green complex. MS, m/z (I_{rel} (%)): 487 $[Cu(\mathbf{1})_2]^+$ (17), 347 $[Cu(\mathbf{1})ClO_4]^+$ (100). IR, ν/cm^{-1}: 3100—3350 br, 1600 (C=N), 1490, 1465, 1430, 1380, 1330, 1315.

X-ray diffraction study of complex 5. The intensities of diffraction reflections were measured at room temperature on an automated CAD-4 single-crystal diffractometer[26] (Cu-Kα radiation, graphite monochromator, ω scanning technique). The unit cell parameters were determined and refined based on 25 reflections in the θ-angle range of 24.79—31.75°. The experimental data set was processed with the use of the WinGX program package.[27] The absorption correction was applied based on ψ scan[28] of six selected reflections. The crystal structure was determined by the Patterson method using the DIRDIF-96 program[29] and refined with anisotropic displacement parameters for all nonhydrogen atoms using the SHELXL-97 program package.[30] In the refinement, the Friedel pairs were not averaged, and the absolute configuration was determined based on the Flack parameter[31] (0.16(6)). The positions of the hydrogen atoms were calculated geometrically and refined using a riding model. The structural data were deposited with the CCDC (refcode 286041).

This study was financially supported by the Russian Foundation for Basic Research (Project No. 04-03-32845) and the Presidium of the Russian Academy of Sciences (Program "Theoretical and Experimental Studies of the Nature of Chemical Bonds and Mechanisms of Chemical Reactions and Processes").

References

1. X.-F. He, C. M. Vogels, A. Decken, and S. A. Westcott, *Polyhedron*, 2004, **23**, 155.
2. H. Sheng-Zhu, S. Dashuang, H. Taishan, W. Jiazhu, H. Zexing, X. Jinlong, and X. Chenghui, *Inorg. Chim. Acta*, 1990, **173**, 1.
3. M. Maji, P. Sengupta, S. K. Chattopadhyay, B. Mostafa, C. H. Schwalbe, and S. Ghosh, *J. Coord. Chem.*, 2001, **54**, 13.
4. B. K. Panda, K. Ghosh, S. Chattopadhyay, and A. Chakravorty, *J. Organomet. Chem.*, 2003, **674**, 107.
5. S. Sengupta, J. Gangopadhyay, and A. Chakravorty, *J. Chem. Soc., Dalton Trans.*, 2003, 4635.
6. J. Gangopadhyay, S. Sengupta, S. Bhattacharyya, I. Chakraboty, and A. Chakravorty, *Inorg. Chem.*, 2002, **41**, 2616.
7. X. Chen, F. J. Femia, J. W. Babich, and J. Zubieta, *Inorg. Chim. Acta*, 2001, **314**, 91.
8. J. L. Corbin and D. E. Work, *Can. J. Chem.*, 1974, **52**, 1054.

9. D. Zhu, Y. Xu, Y. Mei, Y. Sci, C. Tu, and X. You, *J. Mol. Struct.*, 2001, **559**, 119.
10. L. Zhang, L. Liu, D. Jia, and K. Yu, *Struct. Chem.*, 2004, **15**, 327.
11. F. A. Cotton and G. Wilkinson, *Advanced Inorganic Chemistry*, 2nd ed., J. Wiley and Sons, New York, 1966.
12. J. Garcia-Lozano, J. Server-Carrio, E. Coret, J.-V. Folgado, E. Escrivia, and R. Ballesteros, *Inorg. Chim. Acta*, 1996, **75**, 245.
13. S. B. Sanni, H. J. Behm, P. T. Beurskens, G. A. van Albada, J. Reedijk, A. T. H. Lenstra, A. W. Addison, and M. Palaniandavar, *J. Chem. Soc., Dalton Trans.*, 1988, 1429.
14. G. Bernardinelli, G. Hopfgartner, and A. F. Williams, *Acta Cristallogr., Sect. C*, 1990, **46**, 1642.
15. *Organic Electrochemistry*, Ed. M. M. Baiser, Marcel Dekker, New York, 1983.
16. S. Roffia and G. Feroci, *Electroanal. Chem.*, 1978, **88**, 169.
17. Ch. Mann and K. Barnes, *Electrochemical Reactions in Nonaqueous Systems*, Marcel Dekker, New York, 1967.
18. R. Woods, G. A. Hope, and K. Watlong, *J. Appl. Electrochem.*, 2000, **30**, 1209.
19. R. W. Hay, J. A. Crayston, T. J. Cromie, P. Lightfoot, and D. C. L. de Alwis, *Polyhedron*, 1997, **16**, 3557.
20. A. M. Bond, *Modern Polarographic Methods in Analytical Chemistry*, Marcell Dekker, New York, 1980.
21. K. P. Butin, A. A. Moiseeva, E. K. Beloglazkina, Yu. B. Chudinov, A. A. Chizhevskii, A. V. Mironov, B. N. Tarasevich, A. V. Lalov, and N. V. Zyk, *Izv. Akad. Nauk, Ser. Khim.*, 2005, 169 [*Russ. Chem. Bull., Int. Ed.*, 2005, **54**, 173].
22. J. Musie, J. H. Reibenspies, and M. Y. Darsenbourg, *Inorg. Chem.*, 1998, **37**, 302.
23. G. H. Brown and R. Al-Urfali, *J. Am. Chem. Soc.*, 1958, **80**, 2111.
24. D. L. McMasters, R. B. Dunlap, J. R. Kuempel, L. W. Kreider, and T. R. Shearer, *Anal. Chem.*, 1967, **39**, 103.
25. J. J. P. Stewart, *J. Comput. Chem.*, 1989, **10**, 209.
26. *Enraf-Nonius. CAD-4 Software. Version 5.0*, Enraf-Nonius, Delft (The Netherlands), 1989.
27. L. J. Farrugia, *J. Appl. Crystallogr.*, 1999, **32**, 837.
28. A. C. T. North, D. C. Phillips, and F. S. Mathews, *Acta Crystallogr., Sect. A*, 1968, **24**, 351.
29. P. T. Beurskens, G. Beurskens, W. P. Bosman, R. de Gelder, S. Garcia-Granda, R. O. Gould, R. Israel, and J. M. M. Smits, *The DIRDIF-96 Program System. Technical Report*, Crystallography Laboratory, University of Nijmegen (The Netherlands), 1996.
30. G. M. Sheldrick, *SHELXL-97, Program for the Refinement of Crystal Structures*, University of Göttingen, Göttingen (Germany), 1997.
31. H. D. Flack, *Acta Crystallogr., Sect. A*, 1983, **39**, 876.

Received December 24, 2005;
in revised form May 6, 2006